Environ Monit Assess (2019) 191: 162
https://doi.org/10.1007/s10661-019-7296-4

# Deformation of the aquifer system under groundwater level fluctuations and its implication for land subsidence control in the Tianjin coastal region

**Jilong Yang · Guoliang Cao · Dongmei Han · Haifan Yuan · Yunzhuang Hu · Peixin Shi · Yongsheng Chen**

Received: 20 June 2018 / Accepted: 5 February 2019 / Published online: 15 February 2019


**Abstract** This study demonstrates characteristics and mechanisms of deformation of an aquifer system in response to seasonal fluctuations of groundwater level when groundwater pumping has been strictly regulated after experiencing longtime land subsidence. Two boreholes with depth of 1226 m (G2 site) and 905 m (G3 site) were drilled at the Tianjin coastal region where severe land subsidence had occurred since the 1950s. Extensometer/piezometer groups installed at the G2 site illustrate synchronized variations of compaction and groundwater level since 2010 in the aquifer system between depth of 100–400 m which contributes most groundwater pumpage. Monitored land subsidence demonstrates that the shallow aquifer has become the main contributor to the land subsidence, and inelastic compaction still occurred in the aquifers where groundwater level has recovered. Pre-consolidation stresses show that clayey soils in depth < 100 m are under-consolidated, and deep clayey soils show the state of normal- to over-consolidation. The effects of the cyclic groundwater level oscillation on deformation were investigated using repeated loading and unloading tests. Void ratio changes in loading/unloading cycles illustrate that inelastic deformation rate decreases gradually and elastic deformation rate remains almost unchanged with increases of cyclic numbers. The deformation of soil samples from 100 to 400 m is mostly elastic for loading stress in the over-consolidation stress range. These findings suggest that groundwater dewatering in the shallow (depth < 100 m) aquifer will be the primary target to control land subsidence. Groundwater level fluctuations higher than pre-consolidation value in 100–400 m only lead to elastic and recoverable deformation even small residual permanent deformation may continue for a long time. The results improve the understanding of deformation in complex urban aquifers affected by groundwater level fluctuations and highlight the importance of city planning management for controlling land subsidence in coastal cities.

**Keywords** Tianjin coastal region · Clayey soil · Elastic/inelastic deformation · Land subsidence

J. Yang · H. Yuan · Y. Hu · P. Shi · Y. Chen
Tianjin Centre, China Geological Survey, Tianjin 300170, China

J. Yang · H. Yuan · Y. Hu · P. Shi · Y. Chen
CGS Key Laboratory of Muddy Coast Geo-environment, Tianjin 300170, China

G. Cao
State Key Laboratory of Simulation and Regulation of Water Cycle in River Basin, China Institute of Water Resources and Hydropower Research, Beijing 100038, China

D. Han (✉)
Key Laboratory of Water Cycle & Related Land Surface Processes, Institute of Geographic Sciences and Natural Resources Research, Chinese Academy of Sciences, Beijing 100101, China
e-mail: handm@igsnrr.ac.cn

D. Han
College of Resources and Environment, University of Chinese Academy of Sciences, Beijing 100049, China

## Introduction

Land subsidence is a geological hazard mainly due to the over-exploitation of underground fluids by humans

(Galloway and Burbey 2011; Gambolati and Teatini 2015; Ye et al. 2016). Pumping-induced land subsidence is mainly caused by the inelastic compaction of fine-grained clay layers and may also include minor amount of elastic compaction of the coarse-grained sand deposits. The previous maximum effective stress or preconsolidation stress is generally used to define the threshold within which the compaction is elastic (recoverable) and beyond which the compaction is inelastic (unrecoverable) (Galloway and Burbey 2011). The delay flow in thick aquitards can cause ongoing pore pressure declines and residual compaction, resulting continued land subsidence during groundwater level recovery period (Lofgren 1979; Hoffmann et al. 2001; Leake and Galloway 2010). Therefore, cessation of groundwater pumping during a long period generally causes a transition of minor movement from subsidence to uplift (Chen et al. 2007). This indicates that the compaction behavior of the aquifer system may be different with its initial stage after long period of subsidence.

Groundwater pumping has been strictly controlled to mitigate land subsidence in many cities. One of them is the Tianjin coastal region, where the maximum cumulative subsidence in the coastal area has been greater than 3.4 m. Groundwater pumping for municipal water supply has been greatly reduced since 1985 through shifting to surface water. As a result, no further groundwater drawdown occurs and groundwater level mainly shows seasonal cycle oscillation, as influenced by a combination of natural and human factors. However, the characteristics of elastic and inelastic deformation of clay layers in the cyclic loading and unloading caused by this groundwater level variation have not yet been investigated. The groundwater pumping and land subsidence history as well as the thick unconsolidated sediments deposited in the Tianjin coastal region provide a good opportunity for understanding the effects of changes of aquifer characterization on land subsidence.

In this study, the relationship between the elastic and inelastic deformation characteristics of deep clayey soils and land subsidence was systematically studied through analysis of compaction and hydraulic pressure monitoring data at an extensometer/piezometer group and experimental tests of undisturbed soil cores, including consolidation pressure test, and cyclic loading and unloading compaction test. The deep understanding of response of clay layers to groundwater pumping termination or reduction would provide support for effective prevention and control of land subsidence.

## Study area and hydrogeological settings

Tianjin is located in the northeastern part of the North China graben system (Fig. 1). It connects to the Yanshan platform fold belt to the north and the North China fault depression to the south. The grade III tectonic units are divided into Jizhong depression, Cangxian uplift, and Huanghua depression from west to east. These undulating basin-ridge structures were developed from the beginning of the Oligocene and the entire fault depression system was subsiding in the late Quaternary. In the Huanghua depression, unconsolidated sediments have accumulated up to a thickness of 4000–5000 m, forming a material basis for the occurrence of land subsidence (Wang et al. 1994; Bai and Niu 2010). The second and third Quaternary aquifers are the primary source of groundwater in Tianjin.

Groundwater extraction in Tianjin started in the 1920s and had caused severe land subsidence (Fig. 1) (Pan et al. 2004; Yi et al. 2010). Land subsidence was first found in the late 1950s, and the subsidence rate ranged 7–12 mm/year in the central urban area of Tianjin during 1928–1957. Land subsidence in the Tianjin shows an obvious two stages of deformation pattern. Along with extensive exploitation of groundwater, the subsidence rate increased to 30–46 mm/year during 1958–1966, forming several subsidence centers. As the intensity of groundwater exploitation further increased, land subsidence developed rapidly and the subsidence rate reached 80–100 mm/year during 1967–1985. Since 1986, the amount of groundwater exploitation had been reduced to prevent land subsidence through utilizing more surface water (Hu et al. 2002; Dong et al. 2008). The rate of land subsidence in the central urban area and coastal area gradually dropped to 10–15 mm/a. The groundwater level in the second aquifer has recovered ~ 24 m during 1986–1996 and generally stabilized in recent years except dry years such as 2002 (Fig. 2). The land elevation has shown a slight elastic rebound since 1990, which is generally characterized as the post-pumping behavior of the compacted aquifer system (Chen et al. 2007). According to surface deformation revealed by synthetic aperture radar (SAR), the area with subsiding rate of ≥ 50 mm/year

in Tianjin has decreased in recent years compare to that in 2000s, and an uplifting trend exhibits in the main urban area of Tianjin (Zhang et al. 2016; Zhang et al. 2019). The surface rebounding rate ranges from 0 to 20 mm/year during the period of January 2016 to June 2017 (Zhang et al. 2019). This indicates that land subsidence development has been controlled in the urban area of Tianjin. However, the subsiding rate gradually increases from the central urban area of Tianjin to surrounding regions particularly in the north part of Tianjin.

Geothermal water resources development is another important cause of recent land subsidence (Zhang and Jin 1998; Lin et al. 2006). Minghuazhen and Guantao formations are the two porous type geothermal reservoirs in Neogene system (Pang et al. 2012). The geothermal reservoirs of deep Minghuazhen and Guantao formations in Tianjin are generally deposited of normally consolidated sediments (Yang et al. 2014). Large-scale abstraction of geothermal water had started in the end of 1980s, and the total amount of extracted geothermal water was estimated 23.5 million $m^3$ in 2000. Groundwater level in the geothermal reservoir declined 1–5 m annually, which caused severe land subsidence (Minissale et al. 2008). The land subsidence due to geothermal water exploitation in 2005 was estimated to be approximately 5–6 mm/a (Xia et al. 2008). In recent years, to prevent and control haze threat in Tianjin, geothermal resources have been used as a clean energy and the withdrawal of thermal groundwater continues to increase. This has resulted in an increasing trend of land subsidence in the corresponding areas and the subsidence rate has been greater than 50 mm/year in some local seriously affected areas. Injection of cooled water had started at the end of 1990s, and currently, approximately 33% of extracted water has been injected (Duan et al. 2011).

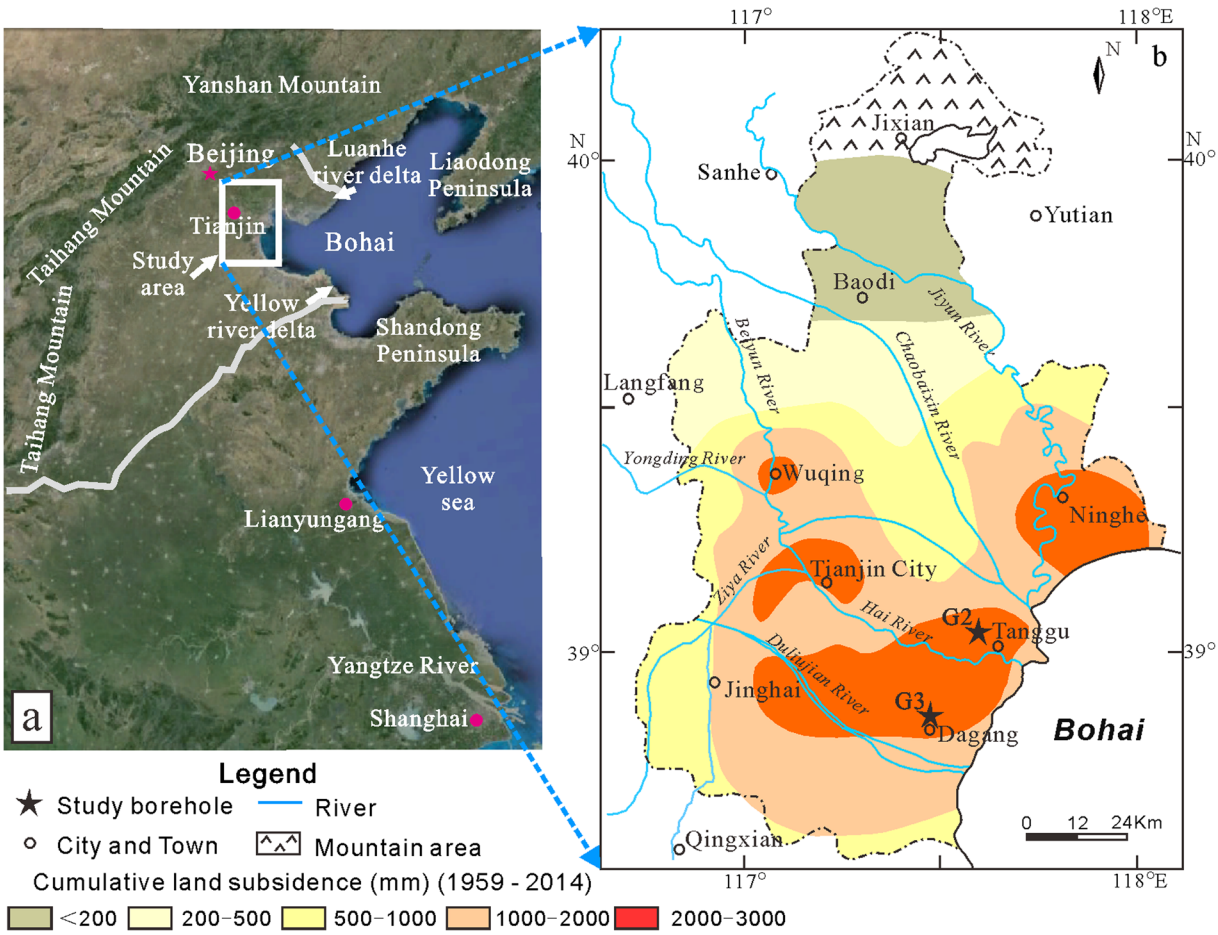


**Fig. 1** **a** Location of Tianjin. **b** Cumulative land subsidence in Tianjin by 2014. The locations of the G2 and G3 boreholes are also shown

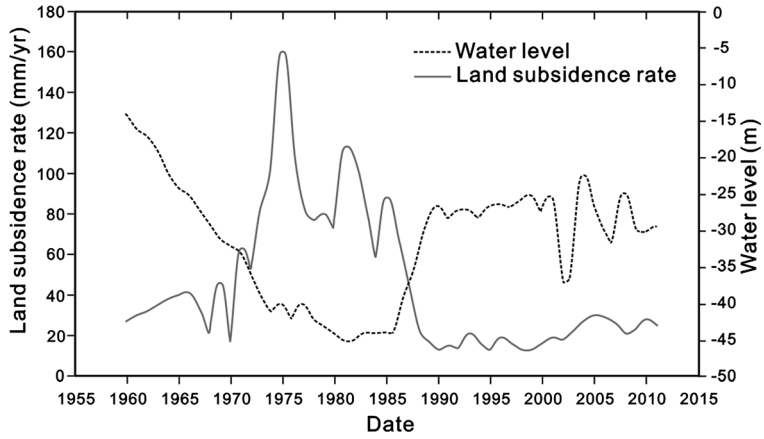


**Fig. 2** Groundwater level fluctuation in the second confined aquifer and varied land subsidence rate in Tianjin (data from Pan et al. 2004; Wang et al. 2015)

## Methodology

### Extensometer/piezometer monitoring

Paired extensometer/piezometer is often used to monitor compaction and fluid pressure at different sediment layers (Zhu et al. 2015). A group of extensometers/piezometers were constructed in 2009 in the Tanggu district located in the Tianjin coastal region (G2 site), with a maximum borehole depth of 1218 m. The G2 borehole is located in the Beitang sag, Huanghua depression. The monitoring system includes one surface mark, eight layerwise mark monitoring points, six underground water level monitoring points, and five clayey soil pore water pressure monitoring points (Fig. 3). Total of 9 extensometers and 5 piezometers were located in the third aquifer which is primary groundwater pumping source in Tianjin. The G2 borehole used in the present study is a pilot hole in the construction of layerwise marks and is used to reveal the stratigraphic structure and engineering mechanical properties. The compaction and water pressure were measured three times per month since July 2011.

According to sediment composition, hydrogeological characteristics, and groundwater exploitation and utilization, the aquifer system in the Tianjin region can be divided into nine confined aquifers across the depth of 1226 m, including four in the Quaternary and five in the upper Neogene (Table 1). The ninth confined aquifer is a Neogene geothermal reservoir which is composed of the lower Neogene Minghuazhen formation and the underlying Guantao formation. The first confined aquifer comprises saline water and is generally not exploited. The remaining confined aquifers comprise freshwater and are exploited to varying degrees. The intensity of groundwater development and utilization varies in different areas. In the Tianjin coastal region, the exploitation of groundwater mainly relies on the second, third, and fourth confined aquifers, and land subsidence has occurred along with exploitation of the second confined aquifer (Yi et al. 2010).

### Aquifer characterization experimental test

In G2, the total thickness of clayey soil reaches 756.9 m and the total thickness of sandy soil is 469.1 m; clayey soil accounts for 61.7% (Table 1, Fig. 3). In this study, 276 undisturbed clayey soil samples were taken from the G2 borehole. For comparison, core sample from another borehole (G3) was also used for experimental tests. The G3 borehole is located in the Qikou sag, Huanghua depression. The G3 borehole can be divided into seven confined aquifers across the depth of 905 m, including four in the Quaternary and three in the upper Neogene. In G3, the total thickness of clayey soil is 513.7 m and the total thickness of sandy soil is 391.3 m; clayey soil accounts for 56.7% (Table 1, Fig. 3). A total of 103 undisturbed clayey soil samples were taken from the G3 borehole. The undisturbed cores were 30 cm in length and 8 cm in diameter. To reduce soil disturbance and prevent soil oxidation and pore

**Fig. 3** Schematic description of the borehole extensometer at G2 site. The lithological profile shows the vertical heterogeneity of the sediments. The locations of extensometer marks and piezometric monitoring points and the screen of groundwater level monitoring wells are also shown. Lithology abbreviations in the lithology legend: SC, silty clay; CS, clayey silt; S, silty sand; FS, fine sand; MS, medium sand

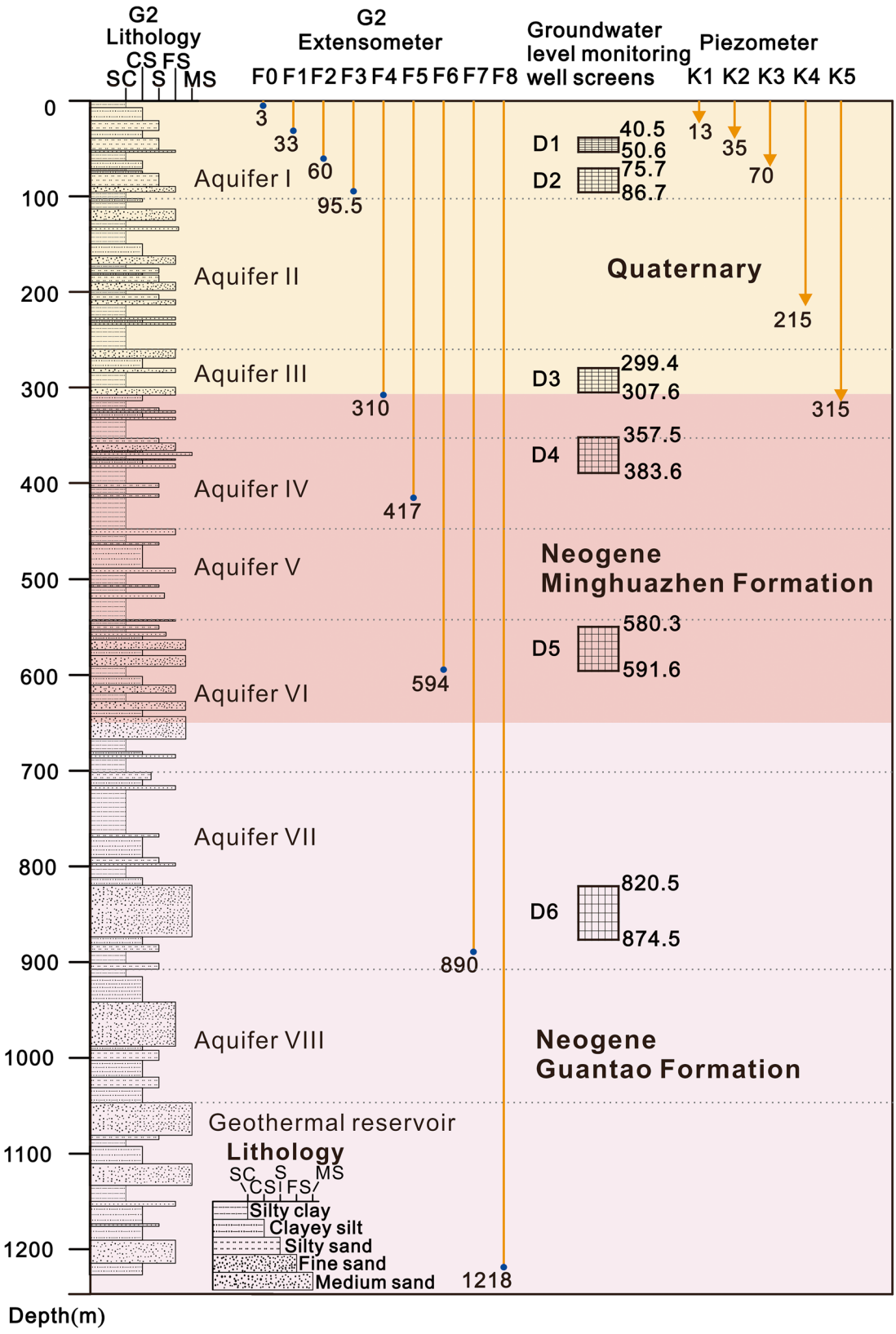
G2 Lithology
CS FS
SC S MS
G2 Extensometer
F0 F1 F2 F3 F4 F5 F6 F7 F8
Groundwater level monitoring well screens
Piezometer
K1 K2 K3 K4 K5
0
100
200
300
400
500
600
700
800
900
1000
1100
1200
Aquifer I
Aquifer II
Aquifer III
Aquifer IV
Aquifer V
Aquifer VI
Aquifer VII
Aquifer VIII
Geothermal reservoir
3
33
60
95.5
310
417
594
890
1218
D1
40.5
50.6
D2
75.7
86.7
13
35
70
215
315
D3
299.4
307.6
D4
357.5
383.6
D5
580.3
591.6
D6
820.5
874.5
Quaternary
Neogene Minghuazhen Formation
Neogene Guantao Formation
Lithology
SC S MS
CS FS
Silty clay
Clayey silt
Silty sand
Fine sand
Medium sand
Depth(m)

**Table 1** Depth of each aquifer and the containing clay thickness for boreholes G2 and G3

| Aquifers | G2 borehole Depth (m) | Clay thickness (m) | Aquifers | G3 borehole Depth (m) | Clay thickness (m) |
|---|---|---|---|---|---|
| Aquifer I | 0–102.5 | 61.96 | Aquifer I | 0–119.7 | 59.1 |
| Aquifer II | 102.5–264.5 | 97.0 | Aquifer II | 119.7–229.0 | 88.0 |
| Aquifer III | 264.5–358.2 | 67.39 | Aquifer III | 229.0–333.2 | 65.0 |
| Aquifer IV | 358.2–447.4 | 63.35 | Aquifer IV | 333.2–438.0 | 42.2 |
| Aquifer V | 447.4–548.3 | 81.65 | Aquifer V | 438.0–562.8 | 81.7 |
| Aquifer VI | 548.3–707.6 | 79.91 | Aquifer VI | 562.8–734.8 | 102.0 |
| Aquifer VII | 707.6–908.3 | 120.3 | Aquifer VII | 734.8–905.0 | 75.7 |
| Aquifer VIII | 908.3–1044.6 | 95.25 | | | |
| Geothermal reservoir | 1044.6–1226.0 | 90.12 | | | |

water evaporation, all soil cores were wrapped with aluminum cover, sealed with wax, and stored at 4–6 °C before analysis. Soil samples were tested for engineering property indices, including moisture content, density, porosity, specific gravity, and grain composition. The gravity stress ($P_0$) was also obtained.

The stratigraphic lithology and grain size composition analysis of G2 and G3 show that the clayey soil thickness is overall larger than the sandy soil thickness (Table 1). The natural moisture content in G2 varies from 10 to 62.8%, with the average of 19.7%, and the natural moisture content in G3 varies from 13.2 to 35.7%, with the average of 19.6%. The clay content in G2 ranges from 0 to 76.1%, with the average of 17.7%, and the clay content in G3 ranges from 0 to 58.2%, with the average of 17.4%.

To investigate the soil pre-consolidation stress, the compression curves (final settlement after compression vs. log normal applied stress) of soil cores in depth less than 100 m were determined with aid of a multistep oedometer with highest applied of stress of 4 Mpa. The compression curves of soil cores deeper than 100 m were obtained with highest applied of stress of 40 Mpa using a material testing machine with greater than 20 t loading. High-pressure consolidation test was conducted on clayey soils in different layers using 66 samples of G2 and 44 samples of G3, and the compression curve was determined for each sample. From the compression curves, the pre-consolidation stresses of clayey soils in the boreholes were obtained graphically using the Casagrande method (Casagrande 1936). The maximum load of repeated loading and unloading test in each soil layer was determined based on the gravity stress and pre-consolidation stress values. The gravity stress was taken as the maximum load of the normally consolidated soils, and the pre-consolidation stress was taken as the maximum load of the over-consolidated soils.

### Cyclic loading consolidation test

The effects of compression stress caused by seasonal oscillation of groundwater level were represented by means of cyclic loading tests. Loading similar to the filed pre-consolidation pressure was applied on prepared specimens. The cyclic loading tests of different layers were conducted using 18 specimens at depth < 500 m of G2 and 13 specimens at depth < 500 m of G3. The compaction pressure was gradually loaded to $P_0$ in four to five steps and kept stable for 24 h, then gradually unloaded. The cyclic loading/unloading tests were carried out four cycles for each specimen. Soil porosity changes were accurately measured during the test to ensure that the results could reveal the characteristics of elastic and inelastic changes in different soil layers during cyclic loading and unloading.

## Results

### Seasonal deformation monitored by extensometers

Extensometers monitored deformation at most marks show inelastic compaction since 2011 (Table 2). The seasonal compaction and rebound measured between F3 to F4 reflect that elastic seasonal deformation superimposed on residual inelastic compaction (Fig. 4). Deformation of the sediments between mark F3 and F4 and changes in pore water pressure in the clay

**Table 2** Monitored deformation at G2 extensometer marks

| Period | Deformation at marks (mm) | | | | | | | |
|---|---|---|---|---|---|---|---|---|
| | F1 | F2 | F4 | F5 | F6 | F7 | F8 | F0 |
| 2011.7–2012.7 | − 28.79 | − 2.44 | 1.34 | − 2.94 | − 1.6 | 1.71 | − 16.2 | − 48.92 |
| 2012.7–2013.7 | − 23.29 | − 1.43 | 0.19 | − 1.74 | − 0.96 | 0.11 | − 5.12 | − 32.24 |
| 2013.7–2014.7 | − 34.02 | − 0.82 | − 1.77 | − 1.01 | − 3.95 | 0.42 | − 4.25 | − 45.4 |
| 2011.7–2014.7 | − 86.1 | − 4.69 | − 0.24 | − 5.69 | − 6.51 | 2.24 | − 25.57 | − 126.56 |

layer (K4) and groundwater level in the aquifer (D3) show synchronized variations (Fig. 4). This indicates that the clay layers between mark F3 and F4 (99.5–310 m depth) are dominated by elastic deformation and the unrecoverable residual compaction is small. The clayey soils in the second and third confined aquifers are dominated by elastic deformation during the monitoring period mainly for the following two reasons. Since the early 1980s, and especially after the implementation of the land subsidence control plan in 1985, the groundwater withdrawal was significantly reduced in the second confined aquifer and groundwater level has obviously recovered. Another reason may be the changes in the internal compaction characteristic of the clayey soils. The clayey soils have been compressed due to rapid groundwater level decline in the 1960s and 1970s and have reached an over-consolidation state (Yang et al. 2014).

## Characteristics of pre-consolidation stress

The concept of over-consolidation ratio (OCR) was used to evaluate the compression state of soils and is defined as the ratio between pre-consolidation stress

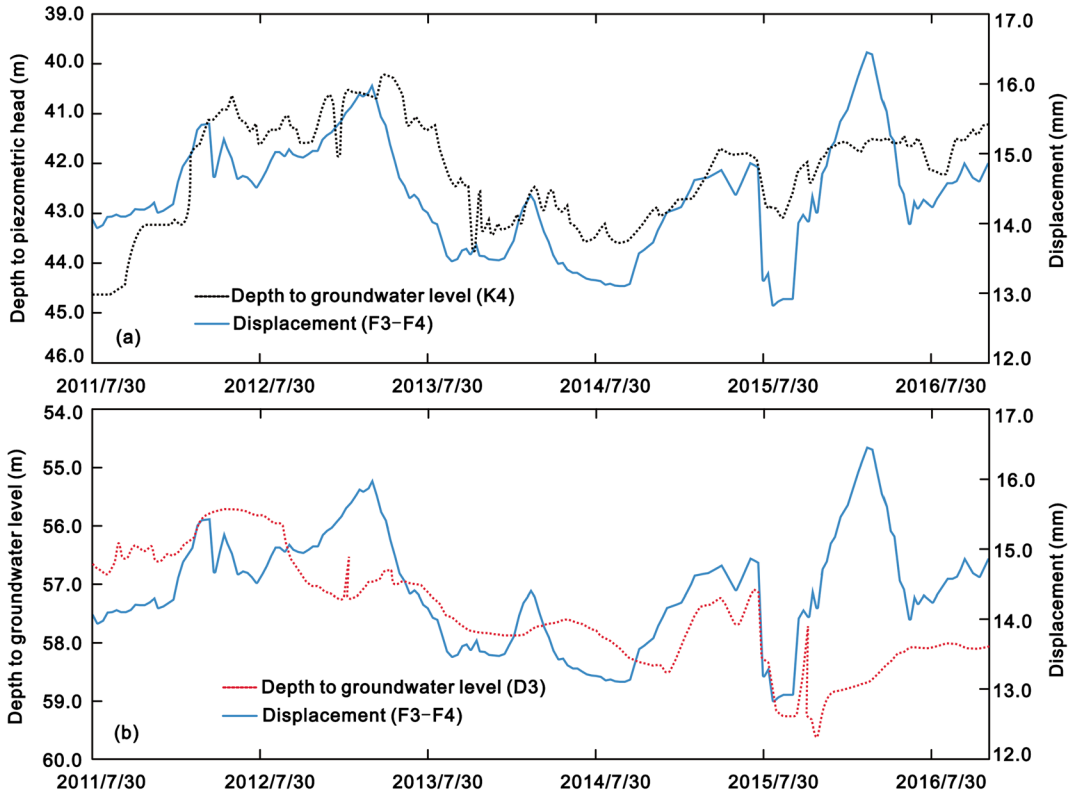


**Fig. 4** Relationship between of **a** piezometric head in the clay layer and **b** groundwater level in the sand layer and the compaction of the second and third confined aquifer (95.5–310 m depth) in G2

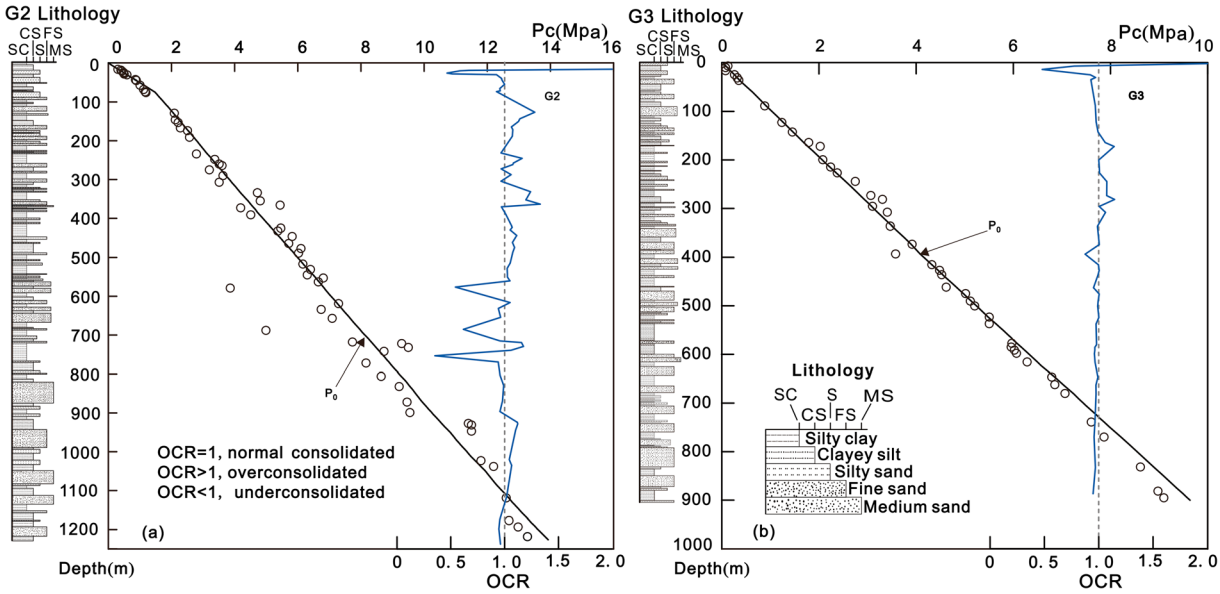


**Fig. 5** Pre-consolidation stress determined through Casagrande method (Casagrande 1936) and variations of OCR with depth for **a** G2 borehole and **b** G3 borehole

($P_c$) and $P_0$. The variations of OCR along depth show the effects of groundwater pumping on the stress status of the sediments. Due to the presence of multilayer marine deposits, soils of G2 in the depth of less than 100 m are characterized by low natural density, high porosity, high moisture content, high compressibility, and under-consolidation, showing the features of soft soil (Fig. 5a). Most of the 100–400 m clayey soils show a state of over-consolidation and slight over-consolidation, mainly due to extensive exploitation of groundwater from the second, third, and fourth confined aquifers in the past. Clayey soils in the depth deeper than 400 m mostly show normal consolidation, but there still exists under-consolidated clay layers in the depth of 600–800 m mainly due to the depositional environment during the formation period (Yang et al. 2014). A state of under-consolidation is where the weight of the overlying sediments and pore water pressure are in disequilibrium and the pore water pressure is higher than the hydrostatic pressure. Under-consolidation is usually caused by high deposition rate and low permeability which are common in alluvial fans and coastal plains (Bryant et al. 1986). Under-consolidation generally exists in the deposition process with pore water pressure dissipation and self-weight consolidation in progress. Considering that the deposition process has finished in million years, soil sample disturbance probably is an important issue affecting the OCR determined in lab. Most soils of G3 in the depth less than 100 m are also under-consolidated and show the features of soft soil. The OCR of soils between 100 and 330 m depth is greater than 1, indicating a state of over-consolidation or slight over-consolidation (Fig. 5b). This is mainly related to the exploitation of groundwater in the second and third confined aquifers and highly consistent with the actual situation in the field. The majority of deep clayey soils in the depth greater than 330 m show normal consolidation, even slight under-consolidation indicating that these soils are generally unaffected by exploitation of groundwater.

The over-consolidated state of the soil in the coastal area is mainly caused by the drop of underground water level (Niu 1998). Due to the drop of underground water level, the osmotic pressure and buoyancy pressure produced by the soil in a certain range are reduced and even disappear. This means that the soil bears a certain additional load within a certain range, resulting in the discharge of pore water from the soil, reduction of pore water pressure, increase of effective stress, and consolidation and compaction of strata. Under certain conditions of water level decline, when the main consolidation of the soil is completed, the depth of the water level can be taken as the critical depth of water level in this soil (Niu 1998; Wang et al. 2006). In the G2 borehole, the 100–300 m soil layers are divided into the second and third confined aquifers in this area. In these two

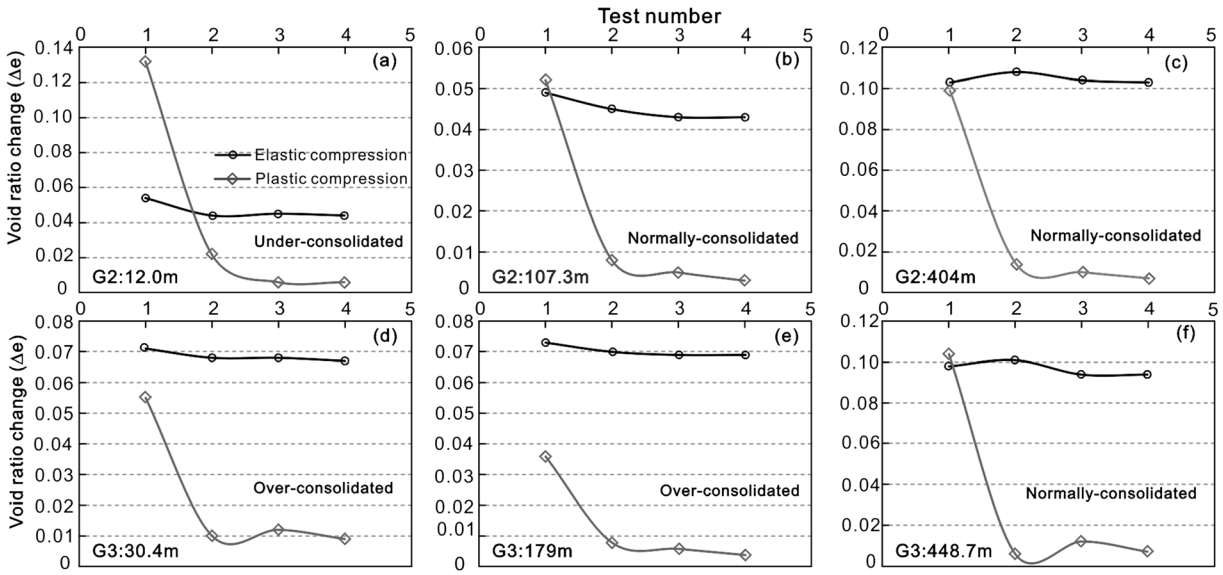


**Fig. 6** Elastic and inelastic deformation in process of cyclic loading and unloading test for samples from **a-c** G2 borehole and **d-f** G3 borehole

aquifers, the soils show a state of slight over-consolidation and over-consolidation, with the over-consolidated value of 0.25–0.45 Mpa and the critical depth of water level at 25–45 m. Based on the layerwise mark and underground water level monitoring results, the current water level is within the critical range and the clayey soil undergoes stage II deformation in the second confined aquifer, so there are synchronous changes of water level and deformation in this aquifer (Fig. 4).

## Role of clayey soils on land subsidence

Because of the storage parameters of clayey soils are stress dependent and generally decrease with increasing effective stress, the deformation caused by same effective stress change will decrease during the compaction progress (Peth and Horn 2006; Galloway and Burbey 2011). The elastic and inelastic displacements converted to void ratios of samples from different depths are plotted with number of loading cycles. The results of 0–$P_0$ cylic loading/unloading test show that the inelastic deformation of the soils decreases gradually with an increasing number of repeated loading and unloading. The void ratio of shallow soil sample in G2 (12 m depth) decreased from 0.132 to 0.011 in the test (Fig. 6a), and the soil sample from depth of 107.3 m decreased from 0.008 to 0.002 (Fig. 6b). Soil sample from depth of 404 m shows greater decreases in void ratio than that from 107.3 m depth (Fig. 6c). Smaller void ratio changes of the soils from the 107.3 m depth indicate great inelastic compaction caused by the past groundwater withdrawal. Soil samples from the G3 borehole show similar variations of void ratio changes with depth (Fig. 6d–f). Most reduction of the inelastic deformation occurred in the first loading test (Fig. 7). The maximum reduction in the inelastic deformation in the first loading test reaches 95%. The elastic deformation generally remains constant, independent of the number of loading and unloading (Figs. 6 and 7).

In the first loading/unloading test step, the elastic and inelastic deformation shows three characteristics: elastic deformation is (1) greater than inelastic deformation for the over-consolidated soil examples (Fig. 6d, e); (2) generally equivalent to inelastic deformation for the normally consolidated soil examples (Fig. 6b–f); and (3) less than inelastic deformation for the under-consolidated soil examples (Fig. 6a). Among the 18 samples of G2, elastic deformation is greater than inelastic deformation in 11 samples, generally equivalent to inelastic deformation in 4 samples and less than inelastic deformation in 3 samples (Fig. 7a). Among the 13 samples of G3, elastic deformation is greater than inelastic deformation in 8 samples, generally equivalent to inelastic deformation in 1 sample and less than inelastic deformation in 4 samples (Fig. 7b). For all soil examples, the inelastic deformation has been

greatly reduced in the following loading/unloading test steps (Figs. 6 and 7). The results reveal that with increasing effective stress, the inelastic deformation will be gradually reduced and the dominated deformation becomes elastic deformation.

The sediments between depth of 0–400 m in Tianjin coastal region show both elastic and inelastic deformation characteristics. The under-consolidated clayey soils in depth of 0–100 m mainly show inelastic deformation, which may produce significant unrecoverable deformation under the external load. For the over-consolidated soils over depth of 100–400 m mainly show elastic deformation, the deformation will show rebound when groundwater level recovers, which is conducive to the restoration of land subsidence. Soils in the depth of 100–400 m of G2 and 100–330 m of G3 are over-consolidated, which show significantly greater elastic deformation than inelastic deformation (Fig. 7a, c). Under the external stress, the soils mainly show elastic deformation, resulting in a positive correlation between elastic deformation and depth. For under-consolidated soils in the shallow and deep parts of G2 and G3, the inelastic deformation is greater than or equal to the elastic deformation (Fig. 7a, c). Under external stress, elastic and inelastic deformation occurs simultaneously, resulting in a lack of significant correlation between elastic deformation and depth. This suggests that land subsidence can be effectively controlled by restoration of groundwater level in the second, third, and fourth confined aquifers in Tianjin coastal region.

It is generally thought the deformation of soils is elastic under applied stress in the over-consolidated stress range. However, the deformation of the normally

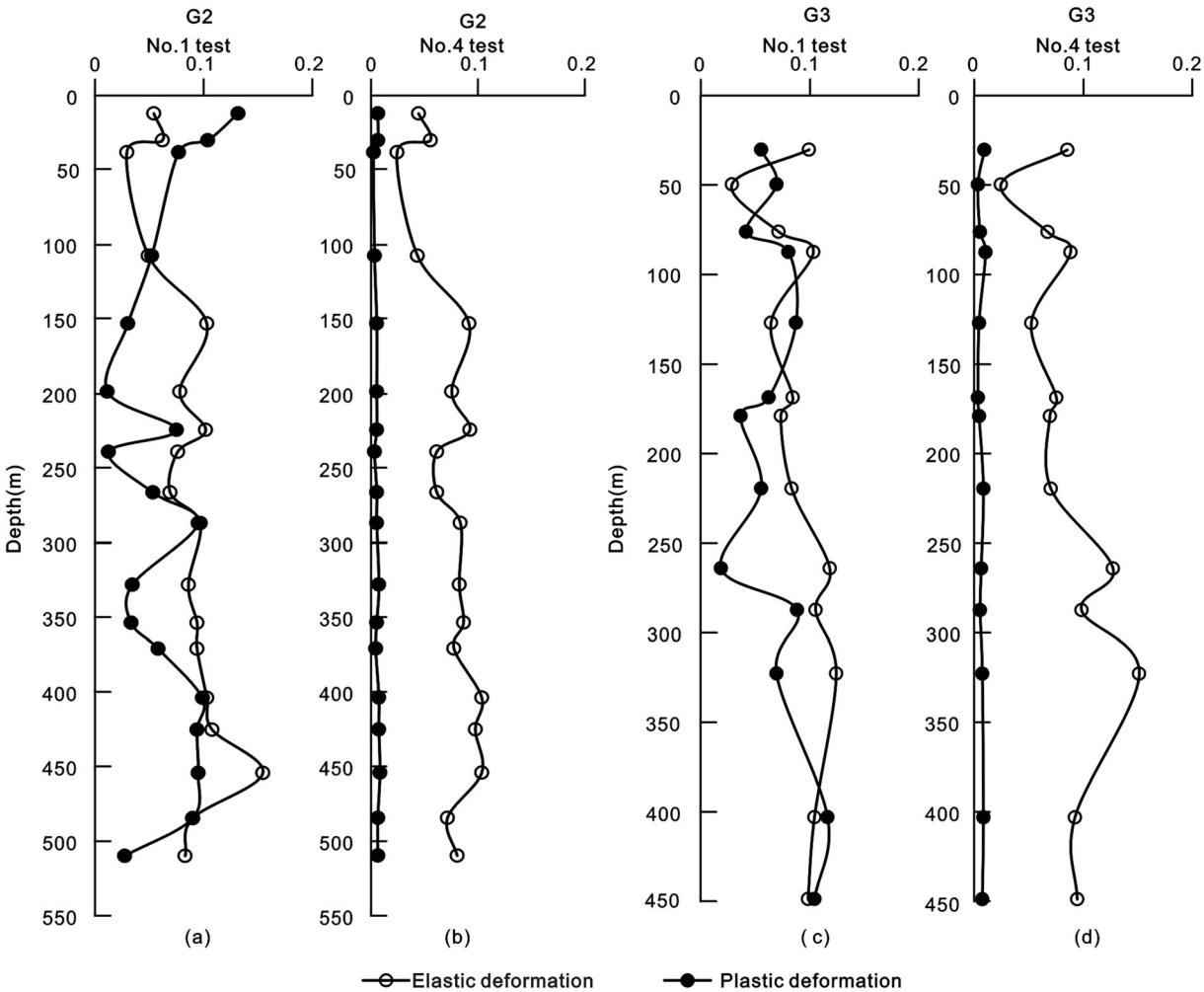


**Fig. 7** Elastic and inelastic deformation in the process of no. 1 and no. 4 repeated for **a-b** G2 borehole and **c-d** G3 borehole

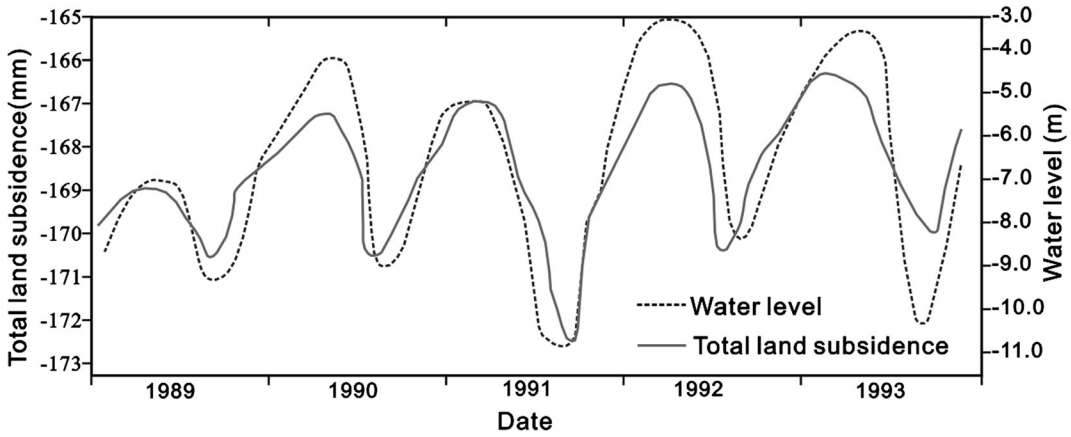


**Fig. 8** Curves related to settlement and water level fluctuation of recharge well in the second confined aquifer (data from Urban geological survey report of Tianjin, unpublished report, 2009)

and over-consolidated specimens is not purely elastic and shows measurable inelastic compaction induced by the cyclic loading. This permanent deformation is partially caused by the destructuring effect of the clayed soils with microstructures (Suddeepong et al. 2015). This perhaps can partially explain the observed permanent compaction of aquifers II–IV.

## Discussion

Under complex geological setting and urban development, land subsidence process is complicated by multiple anthropogenic and natural processes (Terranova et al. 2015). Poro-elastic compaction and rebound of the aquifer system are primary mechanisms controlling the ground deformation. Ground uplift in the main urban area of Tianjin (Zhang et al. 2016; Zhang et al. 2019) and the rebound of the second aquifer during 2011–2013 (Table 2) are triggered by with pore pressure increase associated with groundwater level recovery. This ground uplift phenomenon suggests that groundwater extraction was reduced due to measures implemented to control land subsidence (Hwang et al. 2016) and has also been observed in urban areas such as Naples (Italy) and Phoenix (USA) (Miller and Shirzaei 2015; Coda et al. 2019). The monitored obvious seasonal compaction and rebound of the aquifer system between depth of 100–400 m clearly demonstrated that elastic deformation has become the dominated mechanism. In fact, monitored compression during an in-site artificial recharge test in the central urban area of Tianjin shows synchronous changes in groundwater level and compression in the 1990s when groundwater pumping had been reduced (Fig. 8). The in situ test results are consistent with the cyclic loading test results, which show that the deep clayey soils are acting an elastic system when groundwater level is higher than the pre-consolidation level. As groundwater water level is higher than the lowest point in history, groundwater level drawdown only leads to elastic and recoverable deformation (Chaussard et al. 2017). This suggests that maintaining groundwater level higher than pre-consolidation values (groundwater level in 1980s) would effectively reduce the contribution of the aquifers II–IV to the land subsidence, and these aquifers may still have water supply potential.

The delayed transient groundwater flow in thick clay layer generally results in residual compression and minor rebound during the groundwater level recovery period (Hoffmann et al. 2001; Chen et al. 2007). The synchronized variations of deformation and groundwater level and obvious elastic rebound suggest that the effect of residual compaction is small. The deformation rate is generally highly correlated with the total thickness of the deposits (Ilia et al. 2018), but the delayed compaction is related with the thickness of separate clay layers. Following the one-dimensional vertical consolidation theory by Terzaghi (1925), the average degree of consolidation (the ratio between consolidation at time $t$ and that at the end of the consolidation process) is given by (e.g., Bakr 2015):

$$U(t) = 1 - \frac{8}{\pi^2} \sum_{m=1}^{\infty} \frac{1}{m^2} \exp\left(-m^2 \pi^2 T_v / 4\right) \quad (1)$$

where $m$ is the index of summation, and $T_v$ is dimensionless consolidation time:

$$T_v = \frac{C_v t}{H^2} \quad (2)$$

where $C_v$ is consolidation factor and $H$ is the thickness of the sample. The consolidation factor of clay layers in the Tianjin coastal region is magnitude of $10^{-7}$ $m^2/s$. The maximum thickness of separate clay layers in the G2 is 20–30 m. Approximately 50% of consolidation has occurred after 50 years of groundwater level decline since the 1950s. This indicates that the relatively small compaction of the aquifers II–IV in the groundwater level recovery period since the middle 1980s is attributed to the residual compaction and applying further groundwater drawdowns may cause further compaction.

Groundwater in aquifer I in the Tianjin coastal region is brackish and is rarely pumped for agricultural or industrial usage. Compaction of the clay layers in aquifer I is mostly caused by foundation pit dewatering and load of constructions during the rapid urban development period since 2005 when the Tianjin Binhai New Area (TBNA) was established. Lots of foundation pits in Tianjin are excavated at depth 20–30 m. Monitored compaction at the extensometer mark F1 (33 m depth) accounting for ~ 70% of total land subsidence (Table 2) illustrates that urban development has become the primary contributor to land subsidence in Tianjin costal region. According to variations of consolidation degree with time, only approximately 30% of consolidation has occurred in aquifer I. Compaction of Holocene clay layers is an important contributor to land subsidence in coastal regions (Shirzaei and Bürgmann 2018). However, compaction of the clay layers in the shallow aquifer would cause continuous land subsidence and needs more attention to control land subsidence and protect strategic infrastructures. The complex deformation characteristics of the multilayer aquifer may cause weak correlation between land subsidence and groundwater levels in the primary explored aquifers (Gong et al. 2018). Groundwater artificial recharge would be an effective and applicable method to control compaction of the Neogene aquifers and land subsidence in the Tianjin coastal region (Zheng et al. 2018).

## Summary and conclusions

The land subsidence rate in the Tianjin coastal region has been greatly reduced during the post-pumping period. Characteristics and deformation mechanisms of the aquifer system in response to groundwater level changes after over-exploitation have been investigated through in-site monitoring works and experimental tests. Monitored obvious seasonal rebound and synchronized variations in compaction and groundwater level indicate dominated elastic compaction of the aquifer system between depth of 100–400 m. Most of current land subsidence is associated with compaction of the shallow component of the aquifer at depth < 100 m and the deep component deeper than 400 m mainly caused by geothermal water exploitation. This can be confirmed by the gravity stress and pre-consolidation stress distributions of sediments, which show mainly under-consolidated state in the depth less than 100 m, and normal consolidation in the depth deeper than 400 m. Soils in the depth of 100–400 m show a state of over-consolidation or slight over-consolidation mainly due to extensive exploitation of groundwater in the past.

Accumulation of inelastic compaction is observed at extensometer marks monitoring the deformation of the sediments between depth of 100–400 m. The repeated cyclic loading/unloading tests of soils at different depths show significant decrease of inelastic compression in the first cycle. Inelastic deformation can occur in the loading/unloading cycle even the applied stress in the over-consolidated stress range. These indicate that maintain stable groundwater level higher than pre-consolidation value in aquifers between depth of 100–400 m is necessary to control land subsidence although this may cannot fully eliminate inelastic permanent deformation. Strictly managing groundwater dewatering and applying artificial recharge in the shallow aquifer (< 100 m) and reduction of geothermal water withdrawal from the deep aquifers (> 400 m) can therefore effectively further control land subsidence in the Tianjin coastal region. Improved understanding of deformation mechanism of the complex multilayer aquifer system, monitoring compaction of different strata, and managed city construction are need for controlling land subsidence in coastal urban areas.

**Acknowledgements** This work was supported by the National Key R&D Program of China (2016YFE0102400) and the China Geological Survey Project (#121201006000182401 and #121201006000150009). We thank Changrong Zhao and Sufeng Zhang for sample collection and Tianjin Geological and Mineral Testing Center for assistance with sample testing. We also thank the reviewers for the constructive comments leading to a significant improvement of this manuscript.

## References


Bai, J. B., & Niu, X. J. (2010). Cenozoic consolidation characteristics and land subsidence in Tianjin. *The Chinese Journal of Geological Hazard and Control, 21*, 42–46 (in Chinese with English abstract).

Bakr, M. (2015). Influence of groundwater management on land subsidence in deltas. *Water Resources Management, 29*, 1541–1555.

Bryant, W., Wetzel, A., Taylor, E., Sweet, W. (1986). Consolidation characteristics and permeability of Mississippi Fan sediments. In: Initial Reports Deep Sea Drilling Project, 96, Chapter: Consolidation characteristics and permeability of Mississippi Fan sediments, Editors: A.H. Bouma, J.M. Coleman, et al, pp.797–809.

Casagrande, A. (1936). *The determination of pre-consolidation load and its practical significance. International Conference on Soil Mechanics and Foundation Engineering* (pp. 60–64). Cambridge, MA, July 22–26: Harvard University.

Chaussard, E., Milillo, P., Bürgmann, R., Perissin, D., Fielding, E. J., & Baker, B. (2017). Remote sensing of ground deformation for monitoring groundwater management practices: Application to the Santa Clara Valley during the 2012–2015 California drought. *Journal of Geophysical Research - Solid Earth, 122*, 8566–8582.

Chen, C. T., Hu, J. C., Lu, C. Y., Lee, J. C., & Chan, Y. C. (2007). Thirty-year land elevation change from subsidence to uplift following the termination of groundwater pumping and its geological implications in the Metropolitan Taipei Basin, Northern Taiwan. *Engineering Geology, 95*, 30–47.

Coda, S., Tessitore, S., Martire, D.D., Calcaterra, D., Vita, D.P., Allocca, V. (2019). Coupled ground uplift and groundwater rebound in the metropolitan city of Naples (southern Italy). *Journal of Hydrology*, 569, 470–482

Dong, K.G., Wang, W., Qiang, Y.U., Yang, L.U. (2008). History and enlightenment of land subsidence controlling in Tianjin City. The Chinese Journal of Geological Hazard and Control, 19: 54–59. (in Chinese with English abstract).

Duan, Z., Pang, Z., & Wang, X. (2011). Sustainability evaluation of limestone geothermal reservoirs with extended production histories in Beijing and Tianjin, China. *Geothermics, 40*, 125–135.

Galloway, D. L., & Burbey, T. J. (2011). Review: Regional land subsidence accompanying groundwater extraction. *Hydrogeoly Journal, 19*, 1459–1486.

Gambolati, G., & Teatini, P. (2015). Geomechanics of subsurface water withdrawal and injection. *Water Resources Research, 51*, 3922–3955.

Gong, H., Pan, Y., Zheng, L., Li, X., Zhu, L., Zhang, C., Huang, Z., Li, Z., Wang, H., & Zhou, C. (2018). Long-term groundwater storage changes and land subsidence development in the North China Plain (1971–2015). *Hydrogeoly Journal, 26*, 1417–1427.

Hoffmann, J., Zebker, H. A., Galloway, D. L., & Amelung, F. (2001). Seasonal subsidence and rebound in Las Vegas Valley, Nevada, observed by synthetic aperture radar interferometry. *Water Resources Research, 37*, 1551–1566.

Hu, R., Wang, S., Lee, C., & Li, M. (2002). Characteristics and trends of land subsidence in Tanggu, Tianjin, China. *Bulletin of Engineering Geology and the Environment, 61*, 213–225.

Hwang, C., Yang, Y., Kao, R., Han, J., Shum, C.K., Galloway, D.L., Sneed, M., Hung, W., Cheng, Y., Li, F. (2016). Time-varying land subsidence detected by radar altimetry: California, Taiwan and north China. *Scientific Reports*, 6, 28160.

Ilia, I., Loupasakis, C., & Tsangaratos, P. (2018). Land subsidence phenomena investigated by spatiotemporal analysis of groundwater resources, remote sensing techniques, and random forest method: The case of Western Thessaly, Greece. *Environmental Monitoring and Assessment, 190*, 623.

Leake, S.A., Galloway, D.L. (2010). Use of the SUB-WT package for MODFLOW to simulate aquifer-system compaction in Antelope Valley, California, USA. In: Carreón-Freyre D, Cerca M, Galloway DL (eds) Land subsidence, associated hazards and the role of natural resources development: Proceedings. Eighth International Symposium on Land Subsidence, Santiago de Querétaro, Mexico, 17–22 October 2010, IAHS Publ. 339, pp 61–67.

Lin, L., Zhao, S. M., Dan, L. I., Ma, F. R., & Li, H. J. (2006). A study of the relationship between exploitation of geothermal water in deep-seated aquifers and land subsidence. *Hydrogeology&Engineering Geology, 33*, 34–37 (in Chinese with English abstract).

Lofgren, B.E. (1979). Changes in aquifer-system properties with ground water depletion. Proceedings, International Conference on Evaluation and Prediction of Land Subsidence, Pensacola, December 1978. American Society Civil Engineers, pp: 26–46.

Miller, M. M., & Shirzaei, M. (2015). Spatiotemporal characterization of land subsidence and uplift in Phoenix using InSAR time series and wavelet transforms. *Journal of Geophysical Research - Solid Earth, 120*, 5822–5842.

Minissale, A., Borrini, D., Montegrossi, G., Orlando, A., Tassi, F., Vaselli, O., Huertas, A. D., Yang, J., Cheng, W., Tedesco, D., & Poreda, R. (2008). The Tianjin geothermal field (northeastern China): Water chemistry and possible reservoir permeability reduction phenomena. *Geothermics, 37*, 400–428.

Niu, X.J. (1998). Characteristics of strata consolidation and land subsidence controlling by critical water level. The Chinese Journal of Geological Hazard and Control, 9: 68–74. (in Chinese with English abstract).

Pan, Y., Pan, J. G., Gong, H. L., & Zhao, W. J. (2004). Research on the relation between groundwater exploitation and subsidence in Tianjin proper. *Earth Environment, 32*, 36–39.

Pang, Z., Li, Y., Yang, F., & Duan, Z. (2012). Geochemistry of a continental saline aquifer for $CO_2$ sequestration: The Guantao formation in the Bohai Bay Basin, North China. *Applied Geochemistry, 27*, 1821–1828.

Peth, S., & Horn, R. (2006). The mechanical behavior of structured and homogenized soil under repeated loading. *Journal of Plant Nutrition and Soil Science, 169*, 401–410.

Shirzaei, M., & Bürgmann, R. (2018). Global climate change and local land subsidence exacerbate inundation risk to the San Francisco Bay Area. *Science Advances, 4*, p9234.

Suddeepong, A., Chai, J., Shen, S., Carter, J. (2015). Deformation behaviour of clay under repeated one-dimensional unloading–reloading. *Canadian Geotechnical Journal*, 52, 1035–1044.

Terranova, C., Ventura, G., & Vilardo, G. (2015). Multiple causes of ground deformation in the Napoli metropolitan area (Italy) from integrated Persistent Scatterers DinSAR, geological, hydrological, and urban infrastructure data. *Earth-Science Reviews, 146*, 105–119.

Terzaghi, K. (1925). *Settlement and consolidation of clay* (pp. 874–878). New York: McGraw-Hill.

Wang, M., Lu, Y., Zheng, Y., Wang, W. (2015). A study of the relationship between exploitation of groundwater and land subsidence based on linear regression analysis - in case of Tianjin. *China Water Transport*, 15, 108–110. (in Chinese with English Abstract)

Wang, R., Sun, D., Geng, S., & Hang, Y. (1994). Dynamics of ground subsidence and its effects on geogeaphical environment in Tianjin area. *Acta Geographica Sinica, 49*, 317–323.

Wang, X. Y., Liu, C. L., & Zhang, Y. (2006). Laboratory tests for determination of deformation characteristics of overconsolidated clayey soils and sustainable exploitation groundwater level. *Rock and Soil Mechanics, 27*, 875–879 in Chinese with English abstract.

Xia, D. P., Wang, X. Y., Lin, J. W., Lin, L., & Tian, G. H. (2008). The impact of geothermal development on environmental geology in Tianjin. *Journal of Shandong University of Science and Technology, 27*, 14–18 in Chinese with English abstract.

Yang, J. L., Cao, G. L., Li, H., Li, J., Hu, Y. Z., Xu, Q. M., Qin, Y. F., Du, D., & Cheng, F. (2014). Natural consolidation of late Cenozoic era clay and land subsidence in the Tianjin coastal area. *Rock and Soil Mechanics, 35*, 2579–2586 in Chinese with English abstract.

Ye, S., Xue, Y., Wu, J., Yan, X., & Yu, J. (2016). Progression and mitigation of land subsidence in China. *Hydrogeology Journal, 24*, 685–693.

Yi, L., Zhang, F., Xu, H., Chen, S., Wang, W., & Yu, Q. (2010). Land subsidence in Tianjin, China. *Environment and Earth Science, 62*, 1151–1161.

Zhang, B. M., & Jin, A. S. (1998). Effect of extracting geothermal resources on land subsidence in Binhai area of Tianjin city. *The Chinese Journal of Geological Hazard and Control, 9*, 112–117 in Chinese with English abstract.

Zhang, Y., Wu, H., Kang, Y., & Zhu, C. (2016). Ground subsidence in the Beijing-Tianjin-Hebei region from 1992 to 2014 revealed by multiple SAR stacks. *Remote Sensing, 8*, 675.

Zhang, T., Shen, W. B., Wu, W., Zhang, B., & Pan, Y. (2019). Recent surface deformation in the Tianjin area revealed by Sentinel-1A data. *Remote Sensing, 11*, 130.

Zheng, G., Cao, J. R., Cheng, X. S., Ha, D., & Wang, F. J. (2018). Experimental study on the artificial recharge of semiconfined aquifers involved in deep excavation engineering. *Journal of Hydrology, 557*, 868–877.

Zhu, L., Gong, H., Li, X., Wang, R., Chen, B., Dai, Z., & Teatini, P. (2015). Land subsidence due to groundwater withdrawal in the northern Beijing plain, China. *Engineering Geology, 193*, 243–255.